Published in Turbulence and Anomalous Transport in Magnetized Plasmas (D. Gresillon and M.A. Dubois, eds.), Editions de Physique, Orsay, 293-308 (1987).

Like Particle Transport: A New Theory and Experiments with Pure Electron Plasmas*

T. M. O'Neil, C. F. Driscoll, and D. H. E Dubin
University of California, San Diego
La Jolla, CA 92093

Abstract A new theory of cross-magnetic field transport due to like-particle collisions is presented. The elementary transport step of the new theory is the $\underset{\sim}{E}\times\underset{\sim}{B}$ drift of a particle guiding center which occurs during a binary interaction. The new theory supercedes the traditional theory in the parameter regime where the Debye length is large compared to the Larmor radius ($\lambda_D \gg r_L$), since the flux predicted by the new theory exceeds that predicted by the traditional theory by the ratio $(\lambda_D/r_L)^2 \gg 1$. This parameter regime is standard for magnetically confined pure electron plasmas, and experiments are discussed in which transport of such a plasma toward thermal equilibrium is measured. Preliminary results are consistent with the new theory but not with the traditional theory.

---

*Presented at the international workshop on "Small Scale Turbulence and Anomalous Transport in Magnetized Plasmas" held in Cargèse, Corsica (France), July 1986.

I. Introduction

This talk describes a new theory of cross-magnetic field transport due to like-particle interactions and the consequences of this theory for the transport toward thermal equilibrium of a magnetically confined pure electron plasma. It is well known that under ideal conditions such plasmas can achieve confined thermal equilibrium states.[1] In order to explain experiments now underway at UCSD,[2] it is necessary to consider a hitherto unexamined regime in the theory of like-particle transport: the regime in which $r_L \ll \lambda_D$, where r_L is the electron Larmor radius and λ_D is the electron Debye length. Traditional theories[3,4] of transport due to like-particle collisions were intended to describe ion-ion interactions in neutral plasmas and were formulated for the regime $r_L \gg \lambda_D$. The transport mechanism considered in the new theory yields a particle flux which greatly exceeds that predicted by the traditional theory in the regime $r_L \ll \lambda_D$.[5]

The ratio of the particle flux in the new theory to that in the traditional theory will be seen to be of $O(\lambda_D^2/r_L^2)$ under the assumption that electrons interact only via a Debye-shielded potential. Furthermore, an even larger flux is possible if collective effects are taken into account. However, in the regime of current experiments, theory indicates that the influence of collective effects on the transport is probably negligible.

Experiments are in progress to measure like-particle transport toward thermal equilibrium, and these experiments will be discussed in the last part of the talk. Preliminary measurements of the particle transport have been made as a function of magnetic field. The measured fluxes are orders of magnitude greater than predicted by the traditional theory, scaling approximately as B^{-2} rather than as the predicted B^{-4}. The measured fluxes are, however, consistent with the new theory both in magnitude and in scaling with B. Future experimental measurements may provide detailed tests of the new theory.

II. Transport Mechanism and Scaling

For simplicity, let us consider the case of slab geometry. A pure electron plasma is immersed in a uniform magnetic field $\underset{\sim}{B} = \hat{z}B$, has an electric field and a density gradient in the x-direction [i.e., $\underset{\sim}{E} = \hat{x}E(x)$ and $n = n(x)$], and is homogeneous in the y and z-directions. For simplicity, let us take the temperature, T, to be uniform.

It is useful to start with a fluid description of like-particle transport. The electric field and pressure gradient produce a fluid drift in the y-direction

$$\underset{\sim}{v}(x) = -\frac{c}{B}\left[E + \frac{T}{ne}\frac{\partial n}{\partial x}\right]\hat{y} \quad . \tag{1}$$

Because of viscosity, the shear in this fluid drift gives rise to a force density

$$\underset{\sim}{F}(x) = \frac{\partial}{\partial x}\,\eta\,\frac{\partial v_y}{\partial x}\,\hat{y}\ , \qquad (2)$$

where η is the coefficient of viscosity. In general, this coefficient is of the form $\eta = nm\nu(\Delta x)^2$, where ν and (Δx) are frequency and spatial scales characteristic of the binary interaction which gives rise to the viscosity. In turn, the force density produces a fluid drift in the x-direction, and this drift is the cross-field particle flux

$$\Gamma_x(x) = \frac{-c}{eB}\,\underset{\sim}{F}\times\hat{z}\cdot\hat{x} = \frac{\partial}{\partial x}\,\nu r_L^2(\Delta x)^2\, n\,\frac{\partial}{\partial x}\left[\frac{eE}{T} + \frac{1}{n}\,\frac{\partial n}{\partial x}\right]\ . \qquad (3)$$

As a passing comment, it is worth recalling that the expression for the particle flux in a neutral plasma contains a term which is proportional to the first derivative of the density. This diffusion flux is typically much larger than the higher order flux in Eq. (3). The diffusion flux arises because the electron and ion diamagnetic drifts are in opposite directions, and a collisional drag force between the two species produces a cross-field drift (which is proportional to the plasma density gradient). Of course, this diffusion flux is not present at all for a pure electron plasma.

The quantities ν and Δx must be determined from a microscopic theory. In both the traditional theory and the new theory, ν turns out to be the electron-electron collision frequency. However, the traditional theory and the new theory yield different predictions for Δx, that is, $\Delta x \simeq r_L$ and $\Delta x \simeq \lambda_D$, respectively. Thus, the traditional theory predicts a flux which scales like $\Gamma_x \propto 1/B^4$, and the new theory predicts a flux which scales like $\Gamma_x \propto 1/B^2$.

In the traditional theory, the microscopic treatment is based on a solution of the Boltzmann equation (or, Lenard-Balescu equation) for an inhomogeneous plasma. To understand how the elementary step of the transport process comes about according to this treatment, first recall that the position of a particle guiding center is related to the particle position and particle velocity through the equation

$$\underset{\sim}{r}_g = \underset{\sim}{r} - \frac{\underset{\sim}{v}\times\hat{z}}{\Omega}\ , \qquad (4)$$

where $\Omega = eB/mc$ is the cyclotron frequency. A Boltzmann-like equation treats a collision as a point event; during the collision, $\underset{\sim}{r}$ does not change, but $\underset{\sim}{v}$ undergoes scattering and this produces a step in the guiding center, $\Delta\underset{\sim}{r}_g = -\Delta\,\underset{\sim}{v}\times\hat{z}/\Omega$ (see Fig. 1). From conservation of momentum, one can see the the guiding centers of two like particles make equal and opposite steps, and this is another way to understand why the usual diffusion flux is not present for like-particle transport.

For the purpose of determining Δx in the coefficient of viscosity, the important point to note is that a collision is treated as a point event. The two colliding electrons must have the same value of $\underset{\sim}{r}$; so their guiding centers can be separated by no more than the order of r_L. It is largely this feature which sets $\Delta x \simeq r_L$ in the traditional theory.

The Boltzmann equation picture, where the step in the particle guiding center occurs as a result of a point scattering of the particle velocity vector, makes sense when the range of the force is small compared to the Larmor radius. For example, it makes sense for the case of ion-ion collisions in a neutral plasma, where the Debye length (effective range of the force) is small compared to the ion Larmor radius. On the other hand, for a pure electron plasma (where $\lambda_D \gg r_L$), there are many collisions which are not well described by such a picture.

An example of such a collision is illustrated in Fig. 2. Two electrons approach one another moving in tight helical orbits centered on field lines which are separated by a distance $\rho \sim \lambda_D \gg r_L$. In this situation, the collisional dynamics may be treated by guiding center theory. As the electrons move past one another, they undergo equal and opposite $\underset{\sim}{E} \times \underset{\sim}{B}$ drifts, where $\underset{\sim}{E}$ is the interaction field. There is very little velocity scattering for such a collision, and the Boltzmann analysis completely underestimates the size of the guiding center steps. For the purpose of estimating Δx in the coefficient of viscosity, the important point to note is that the two guiding centers can be separated by as much as λ_D; so such collisions lead to a $\Delta x \simeq \lambda_D$. Since $\lambda_D \gg r_L$, these large impact parameter collisions (i.e., $\rho \sim \lambda_D \gg r_L$) provide the dominant contribution to the viscosity.

III. Guiding Center Model of the BBGKY Hierarchy

To obtain a kinetic theory which treats such collisions, we construct a guiding center model of the BBGKY hierarchy.[5] In this model, the state of each electron is specified by its three configuration coordinates and its axial velocity (x, y, z, v). From the 1-electron equation of the hierarchy (or simply from inspection), one can see that the particle flux in the x-direction is given by

$$\Gamma_x(x) = -\int dv_1 \int dv_2 \int d^3\underset{\sim}{r}_2 \left(\frac{c}{B}\right)\frac{\partial \psi}{\partial y_1}\left(\underset{\sim}{r}_1, \underset{\sim}{r}_2\right) f_2\left(\underset{\sim}{r}_1, v_1, \underset{\sim}{r}_2, v_2, t\right) \qquad (5)$$

where $\psi(\underset{\sim}{r}_1, \underset{\sim}{r}_2)$ is the interaction potential between electrons 1 and 2 and $f_2(\underset{\sim}{r}_1, v_1, \underset{\sim}{r}_2, v_2, t)$ is the 2-electron distribution function.

For simplicity, we first treat the shielding in an ad-hoc manner and write $\psi(\underset{\sim}{r}_1, \underset{\sim}{r}_2)$ as the Debye-shielded Coulomb interaction

$$\psi\left(\underset{\sim}{r}_1, \underset{\sim}{r}_2\right) = \frac{-e}{\left|\underset{\sim}{r}_1 - \underset{\sim}{r}_2\right|} \exp\left[-\frac{1}{\lambda_D}\left|\underset{\sim}{r}_1 - \underset{\sim}{r}_2\right|\right], \qquad (6)$$

where $1/\lambda_D^2 = 4\pi e^2 n[(x_1 + x_2)/2]/T$. This treatment avoids the mathematical complexities associated with the development of shielding in an inhomogeneous plasma. A proper treatment has been completed and the results will be presented below.[6] In accord with the ad-hoc treatment of shielding, the 2-electron distribution evolves according to the equation

$$\left\{\frac{\partial}{\partial t} + (v_2 - v_1)\frac{\partial}{\partial z_2} + \frac{c}{B}[E(x_1) - E(x_2)]\frac{\partial}{\partial y_2} + \frac{e}{m}\frac{\partial \psi}{\partial z_2}\left(\frac{\partial}{\partial v_2} - \frac{\partial}{\partial v_1}\right)\right.$$

$$\left. + \frac{c}{B}\frac{\partial \psi}{\partial y_2}\left(\frac{\partial}{\partial x_1} - \frac{\partial}{\partial x_2}\right) + \frac{c}{B}\left(\frac{\partial \psi}{\partial x_2} - \frac{\partial \psi}{\partial x_1}\right)\frac{\partial}{\partial y_2}\right\} f_2 = 0 \quad . \tag{7}$$

Here, use has been made of the assumed homogeneity in y and z.

This equation can be solved by use of a perturbation expansion in the strength of the interaction, ψ. To this end, we set $f_2 = f_2^{(0)} + f_2^{(1)}$ and $L = L^{(0)} + L^{(1)}$, where L is the operator which acts on f_2. The superscript (0) refers to quantities which are zero order in ψ and the superscript (1) to quantities which are first order in ψ. Thus, $L^{(0)}$ consists of the first three terms in the bracket of Eq. (7) and $L^{(1)}$ consists of the last three terms.

In zero order, Eq. (7) reduces to $L^{(0)} f_2^{(0)} = 0$, which has the solution $f_2^{(0)} = f_2^{(0)}(x_1, v_1, x_2, v_2)$. The solution is further constrained by the observation that in zero order there can be no electron-electron correlations; so the 2-electron distribution must reduce to a product of 1-electron distributions. Taking the 1-electron distribution to be a Maxwellian characterized by density n(x) and temperature T yields the solution

$$f_2^{(0)} = \frac{n(x_1)\, n(x_2)}{(2\pi T/m)} \exp\left[-\frac{1}{T}\left(\frac{mv_1^2}{2} + \frac{mv_2^2}{2}\right)\right] . \tag{8}$$

It is interesting to note that the Maxwellian character of the distribution is forced by collisions which are not directly included in the guiding center model. This model focuses attention on the large impact parameter collisions (i.e., $\rho \sim \lambda_D >> r_L$) which yield the dominant contribution to the flux. Velocity scattering, which forces the distribution to be Maxwellian, is associated mainly with small impact parameter collisions (i.e., $\rho \leq r_L$). These collisions are not directly included in the guiding center model but do have the indirect effect of forcing the distribution to be Maxwellian.

In first order, Eq. (7) reduces to the form $L^{(0)} f_2^{(1)} + L^{(1)} f_2^{(0)} = 0$. By observing that $L^{(0)} = d/dt$ is the total time derivative along unperturbed orbits and that

$$\frac{d\psi}{dt} = (v_2 - v_1)\frac{\partial \psi}{\partial z_2} - \frac{c}{B}[E(x_2) - E(x_1)]\frac{\partial \psi}{\partial y_2} , \tag{9}$$

the solution can be written as

$$f_2^{(1)} = \frac{e\psi}{T} f_2^{(0)} + [v_y(x_1) - v_y(x_2)] f_2^{(0)} \frac{e}{T} \int_{-\infty}^{t} dt' \left(\frac{\partial \psi}{\partial y_2}\right)' \quad , \tag{10}$$

where $v_y(x)$ is the fluid velocity introduced in Eq. (1) and the time integral is taken over unperturbed orbits. This equation has a simple physical interpretation. The first term on the right is the thermal equilibrium correlation function established as electrons 1 and 2 stream along the field lines. The second term is the perturbation in that function produced by shears in $v_y(x)$. As one would expect, it is only the second term which contributes to the flux.

Substituting $f_2 = f_2^{(0)} + f_2^{(1)}$ into Eq. (5) and writing out $v_y(x)$ in terms of the electric field and density gradient yields the expression

$$\Gamma_x(x_1) = \int d^3r_2 \left\{ \left[\frac{1}{n(x_2)} \frac{dn}{dx_2} - \frac{1}{n(x_1)} \frac{dn}{dx_1} \right] + \frac{e}{T}[E(x_2) - E(x_1)] \right\} n(x_1)\, n(x_2)\, h(\underset{\sim}{r}_2 - \underset{\sim}{r}_1,\ (x_1 + x_2)/2) \ , \tag{11}$$

where

$$h[r_2 - r_1,\ (x_1 + x_2)/2] = \int dv_1 \int dv_2 \frac{\exp\left[-T^{-1}\left(\frac{1}{2}mv_1^2 + \frac{1}{2}mv_2^2\right)\right]}{(2\pi T/m)} \int_{-\infty}^{t} dt' \left(\frac{c}{B}\right)^2 \left(\frac{\partial \psi}{\partial y_2}\right)\left(\frac{\partial \psi}{\partial y_2}\right)' . \tag{12}$$

Because of Debye shielding, the r_2 integral in Eq. (11) receives significant contributions only for x_2 near x_1 (i.e., for $|x_2 - x_1| \leq \lambda_D$). We assume that $n(x_2)$ and $E(x_2)$ vary on a length scale which is large compared to λ_D, and we make Taylor expansions of $n(x_2)$ and $E(x_2)$ about $x_2 = x_1$. The variation of $h[\underset{\sim}{r}_2 - \underset{\sim}{r}_1,\ (x_1 + x_2)/2]$ through its second argument is on the same scale as that for $n(x_2)$ and $E(x_2)$; so $h[\underset{\sim}{r}_2 - \underset{\sim}{r}_1,\ (x_1 + x_2)/2]$ also can be Taylor expanded about $x_2 = x_1$. Of course, the dependence of $h[\underset{\sim}{r}_2 - \underset{\sim}{r}_1,\ (x_1 + x_2)/2]$ on its first argument cannot be Taylor expanded; it is the peaked nature of this dependence which justifies the other expansions. Carrying out the expansions and substituting into Eq. (11) yields the result

$$\Gamma_x(x_1) = \frac{d}{dx_1} n^2(x_1) K(x_1) \frac{d}{dx_1} \left[\frac{1}{n(x_1)} \frac{dn}{dx_1} + \frac{e}{T} E(x_1) \right] \ , \tag{13}$$

where $K(x_1) = \int d^3\underset{\sim}{r}\, (x^2/2) h(\underset{\sim}{r}, x_1)$ is the transport coefficient and $\underset{\sim}{r} = \underset{\sim}{r}_2 - \underset{\sim}{r}_1$ is the relative position vector.

The unperturbed orbit for the relative position vector is specified by

$$z' = z + v(t' - t),$$

$$y' = y + (c/B)[E(x_2) - E(x_1)](t' - t),$$

and $x' = x$. Here, the relative velocity $v = v_2 - v_1$ and x_1 and x_2 are independent of t'. By use of the relation

$$|E(x_2) - E(x_1)| \leq |dE/dx_2|\lambda_D = 4\pi en\lambda_D ,$$

one can see that the inequality $\lambda_D \gg r_L$ implies the inequality $\bar{v} \gg (c/B)|E(x_2) - E(x_1)|$. In other words, for most collisions, the relative velocity parallel to the field is much larger than the relative velocity across the field. As a first approximation, we neglect the relative cross-field motion which occurs during an interaction and set $y' \simeq y$.

By use of the orbit $z' = z + v(t' - t)$, $y' = y$, and $x' = x$ together with a Fourier representation of the interaction potential

$$\psi = \int \frac{d^3k}{(2\pi)^3} \frac{(-4\pi e)}{k^2 + 1/\lambda_D^2(x_1)} \exp(i\underset{\sim}{k} \cdot \underset{\sim}{r}) , \tag{14}$$

one can show that

$$K(x_1) = \frac{\pi e^2 c^2 \lambda_D^2(x_1)}{6B^2} \int \frac{dv}{|v|} \frac{\exp(-mv^2/4T)}{(4\pi T/m)^{1/2}} . \tag{15}$$

Here, the integral over the relative velocity arises in the following way. The integral $\int dv_1 \int dv_2$ is replaced by the integral $\int dv \int dV$, where $V = (v_1 + v_2)/2$ is the center-of-mass velocity, and then the integral over the center-of-mass velocity is carried out.

The integral over the relative velocity is logarithmically divergent at $v = 0$. Physically, this corresponds to the fact that two electrons with small relative velocity interact for a long time and experience large $\underset{\sim}{E} \times \underset{\sim}{B}$ steps. To remove the divergence we must take into account physical effects which limit the time of the interaction, or, equivalently, cut off the velocity integral at some small but finite value of $|v|$ (i.e., $\min|v| = \Delta v$).

One such effect is small-angle scattering. The small-impact-parameter collisions, which are not directly included in the guiding-center model, produce a diffusive spreading of $v = v_2 - v_1$. During the time τ, the amount of spreading is $(\Delta v)^2 = \nu \bar{v}^2 \tau$, where ν is the collision frequency and $\bar{v}^2 = T/m$. This velocity spread can separate electrons 1 and 2 by a Debye length during the time τ provided that $(\Delta v)\tau = \lambda_D$. Eliminating τ between the two relations yields the result $(\Delta v/\bar{v}) = (\nu/\omega_p)^{1/3}$, where ω_p is the plasma frequency.

A competing effect is associated with the relative cross-field motion of the two electrons. Two electrons for which $|x_1 - x_2| \simeq \lambda_D$ have a relative y velocity of $(c/B)|dE/dx|\lambda_D = (c\lambda_D 4\pi en)/B$. The time τ for this relative velocity to produce a separation $|y_1 - y_2| \simeq \lambda_D$ is given by

$\tau(4\pi enc)/B = 1$. Relating this time to a relative parallel velocity through $(\Delta v)\tau = \lambda_D$ yields the result $(\Delta v/\bar{v}) = r_L/\lambda_D$. Of course, the cutoff for the velocity integral in Eq. (15) is determined by the effect which yields the largest value of $(\Delta v/\bar{v})$.

Introducing the cutoff and carrying out the velocity integral yields the result

$$K(x_1) = \frac{\sqrt{\pi}\, e^2 c^2 \lambda_D^2(x_1)}{6B^2\bar{v}} \ln\left[\frac{\bar{v}}{\Delta\bar{v}}\right] \tag{16}$$

This coefficient should be compared to the coefficient obtained previously, that is, to $(3/8)(\nu/n)r_L^4$, where $\nu = (16\sqrt{\pi}\, e^4 n/15\, m^2\bar{v}^3)\ln(r_L/b)$ is the collision frequency and $b = e^2/m\bar{v}^2$ is the distance of closest approach.[3] The ratio of the new coefficient to the previous coefficient is given by

$$\left(\frac{5}{12}\right)[\ln(\bar{v}/\Delta v)/\ln(r_L/b)]\,(\lambda_D/r_L)^2 \quad .$$

The analysis also has been performed without making an ad-hoc assumption of shielding.[6] The plasma dielectric is treated properly, and the shielding arises naturally through the plasma response. One finds that the flux can be written as the sum of two parts

$$\Gamma_x = \Gamma_x)_{\text{shielded}} + \Gamma_x)_{\text{modes}} \quad , \tag{17}$$

where the first term is due to the shielded interaction and is to within a factor of 2 equal to the result given by Eqs. (13) and (16). The second term is due to the interaction of electrons 1 and 2 through weakly damped modes. Electron 1 Cerenkov radiates a mode which propagates some distance across the plasma and then is absorbed by electron 2.

In this way, a large interaction length can occur (i.e., $\lambda_D \ll \Delta x < L$, where L is the plasma dimension). Of course, the effective interaction frequency scales inversely with the interaction length (i.e., $\nu \propto \gamma = v_g/\Delta x$); so the contribution to the viscosity scales like the first power of the interaction length [i.e., $\nu(\Delta x)^2 \propto \Delta x$]. It turns out that the most important modes are those with $\Delta x \sim L$, and the magnitude of the total contribution from these modes is of order

$$\left|\frac{\Gamma_x)_{\text{modes}}}{\Gamma_x)_{\text{shielded}}}\right| \sim f\,\frac{L}{\lambda_D} \tag{18}$$

where the factor f arises from the sum over modes and is small (i.e., $f \sim 10^{-2} - 10^{-3}$).

Thus, the contribution from the weakly damped modes is negligible, unless the plasma is large (i.e., $L \geq \lambda_D/f$). Note that for a pure electron plasma the ratio of the potential difference across the plasma to the

temperature is of order $e\Delta\varphi/T \sim (L/\lambda_D)^2$. For the experiments to be discussed next, the effect of weakly damped modes is quite negligible (i.e., $L \ll \lambda_D/f$), but their effect may be important for future experiments with cryogenic pure electron plasmas.[7]

IV. Experiments

Let us now turn to a discussion of the pure electron plasma experiments.[2,7] A schematic diagram of the confinement geometry is shown in Fig. 3. The entire apparatus is in a uniform magnetic field, $\underset{\sim}{B} = \hat{z}B$, and is evacuated to below 10^{-10} Torr. The system is repetitively pulsed in the following sequence. Initially, cylinders A and B are held at ground potential, and cylinder C is biased strongly negative. Electrons emitted from a negatively biased thermionic source then form a column from the source through cylinder B. When cylinder A is biased negative, a portion of the electron column is trapped in the region of cylinder B. The electrons are confined radially by the magnetic field and are confined axially by the electrostatic fields. Because the column is unneutralized, there is a radial electric field. This field and the radial pressure gradient produce a drift rotation of the plasma and also drive a slow radial transport.

After a time t has elapsed, cylinder C is pulsed to ground potential and the electrons stream out along the field lines to collimators, velocity analyzers, and collectors. Repetition of the cycle many times allows one to construct the radial density and temperature profiles as a function of time. This relies on shot to shot reproducibility, which is typically better than 1%.

Typical values of the density, temperature, and magnetic field strength are

$$n \simeq 10^7 \text{ cm}^{-3}, \quad T \simeq 1 \text{ eV}, \quad B \simeq 100 \text{ Gauss},$$

and typical values of the Larmor radius, Debye length, and plasma radius are

$$r_L \simeq 0.02 \text{ cm}, \quad \lambda_D \simeq 0.2 \text{ cm}, \quad r_p \simeq 2 \text{ cm}.$$

One can see that these values are consistent with the length scale ordering assumed in the theory. Typical values of the cyclotron frequency, plasma frequency, axial bounce frequency, rotation frequency, collision frequency, and inverse transport time are

$$\nu_c \simeq 3\times 10^8 \text{ sec}^{-1}, \quad \nu_p \simeq 3\times 10^7 \text{ sec}^{-1}, \quad \nu_R \simeq \nu_B \simeq 10^6 \text{ sec}^{-1},$$

$$\nu \simeq 200 \text{ sec}^{-1}, \quad (1/\tau)_{\text{Trans.}} \simeq 1 \text{ sec}^{-1}.$$

One can see that there is a comfortable separation between the time scales for collective phenomena, collisions, and transport.

The plasma comes to thermal equilibrium in two stages. First, collisions produce a local thermal equilibrium along each field line on a time scale $\nu^{-1} \simeq (200)^{-1}$ sec. On a much longer time scale, $\tau_{Trans.} \simeq 1$ sec, cross magnetic field transport allows the plasma to come to a global thermal equilibrium.

It is easy to write down the electron distribution function for a state of global thermal equilibrium.[1] Here, we switch briefly from guiding center distributions to electron distributions (in 6-dimensional phase space). Since the confinement geometry has cylindrical symmetry, at least nominally, the canonical angular momentum for an electron enters the distribution on equal footing with the Hamiltonian for the electron. The Boltzmann distribution is replaced by a distribution of the form

$$f = n_o \left(\frac{m}{2\pi T}\right)^{3/2} \exp\left[-\frac{1}{T}(H - \omega_R P_\theta)\right] , \tag{19}$$

where

$$H = \frac{mv^2}{2} - e\varphi(r,z)$$

$$P_\theta = mv_\theta r - \frac{e}{c} A_\theta(r) r . \tag{20}$$

Here, $\varphi(r,z)$ is the electric potential and $A_\theta(r,z) = Br/2$ is the vector potential for a uniform axial magnetic field. (The diamagnetic field is negligible for the low electron densities and velocities considered here.) The three parameters n_o, T, and ω_R are determined by the total number of electrons, energy, and canonical angular momentum in the system. It is quite easy to rewrite distribution (19) so that the velocity dependence is Maxwellian in a frame rotating with angular velocity ω_R. In other words, the distribution describes a plasma of electrons which rotates without shear (rigid rotation) with angular velocity ω_R.

It is easy to see that distribution (19) corresponds to a confined set of electrons. The electric potential becomes large and negative near the negatively biased end cylinders; so the distribution is exponentially small at the ends. For sufficiently large magnetic field, the vector potential forces the distribution to be exponentially small at large values of r, and the cylindrical wall is assumed to be outside this radius.

The existence of such confined thermal equilibrium states is a unique property of totally unneutralized plasmas. It is well known that a neutral plasma cannot be confined by static electric and magnetic fields and also be in a state of global thermal equilibrium; if it could the controlled fusion problem would be trivial. It is precisely the fact that a confined neutral plasma is never in thermal equilibrium which means that there is always free energy to drive instabilities. In contrast, distribution (19) describes a plasma which is in a state of minimum free energy. In principle, such a plasma is guaranteed to be stable and to be confined forever.

In practice, life is more difficult. A real confinement apparatus does not have perfect cylindrical symmetry; so the total canonical angular momentum is not really constant. Small field errors and construction errors break the symmetry and apply a small torque on the plasma, and this allows the plasma to expand slowly in radius.[7] However, by carefully minimizing such effects, quite long confinement times can be achieved. For example, pure electron plasmas are routinely confined for a day.[8] For the experiments to be described here, the plasma radius doubles on a time scale of 10^2-10^3 sec. Since this is much longer than the time for transport to thermal equilibrium (i.e., $\tau_{Trans.} \simeq 1$ sec), we will neglect the effect of the external torque.

Since the electric potential is largely determined by the electrons themselves, one must solve for the potential self-consistently. One must solve Poisson's equation with the charge density given by the velocity integral of distribution (19). This can be done for the full three-dimensional geometry,[1] but the results are easiest to display for the case of a long column, where the radial density profile is the significant feature. Fig. 4 displays a family of such profiles, and the asterisk marks the profile which is closest to the experimental parameters.

In general, the density and temperature profiles of the injected plasma do not correspond to thermal equilibrium. The radial electric field and pressure gradient give rise to a fluid drift velocity in the azimuthal direction

$$v_\theta(r) = \frac{c}{B}\left[+\frac{\partial\varphi}{\partial r} - \frac{1}{ne}\frac{\partial}{\partial r}(nT)\right] , \qquad (21)$$

which in general does not correspond to rigid rotation (i.e., $v_\theta(r)/r \neq$ constant). Viscous forces in the azimuthal direction then produce a radial drift: the particle flux

$$\Gamma_r(r) = -\frac{1}{r^2}\frac{\partial}{\partial r} r^2 \eta \frac{c}{eB} r \frac{\partial}{\partial r}\left(\frac{v_\theta(r)}{r}\right) . \qquad (22)$$

This flux conserves not only total particle number but also the total canonical angular momentum. One can see that the flux vanishes for rigid rotation. In fact, simply by setting $v_\theta(r)/r$ and $T(r)$ equal to constants in Eq. (21), one obtains an equation for $\partial n/\partial r$ which leads to the thermal equilibrium density profile.*

In Eqs. (21) and (22) we have included drifts due to temperature gradients in the manner suggested by fluid theory, i.e. as arising from $\partial(nT)/\partial r$. We should emphasize, however, that this form has not been obtained directly from the guiding center analysis of the new theory. In the current

---

*To be precise, one must include in Eq. (21) a drift due to the centrifugal force. This is typically small for the experimental parameters and has been neglected in the discussion of transport.

experiments, the effect of the temperature gradient is smaller than that of the density gradient, i.e. $(1/T)\left|dT/dr\right| < (1/n)\left|dn/dr\right|$. However, the temperature gradient is generally not negligible as was assumed in the theoretical discussion.

Finally, let us turn to a discussion of the experimental data. Beyond cylinder C there is a plate with a small hole that can be moved radially (the collimator). With a charge collector behind the hold, we obtain a signal $Q(r)$ proportional to the number of electrons on the field lines passing through the hole. Additionally, a "Beach Analyzer" (parallel velocity discrimination in the presence of a secondary magnetic field) is used to obtain the perpendicular temperature of the electrons. Fig. 5 shows an early example of such measurements as a function of radius for a plasma at $t = 0$.

The number of electrons is maximal at $r = 0$, and falls to zero at about $R_w/2$. The plasma temperature in this case is about 1 eV in the center and rises to 1.8 eV at the plasma edge. Presently, the shot-to-shot variation in $Q(r)$ are typically $\pm 1\%$, the temperatures are measured to $\pm 10\%$, and the zeroing problems apparent in Fig. 5 have been eliminated.

We obtain the density $n(r,z)$ from the measured z-integral $Q(r)$ by numerically solving a 2-dimensional Poisson equation. Because the electrons are in local thermal equilibrium along each field line, the z-dependence of the density is given by the Boltzmann factor

$$n(r,z) = n(r,0) \exp\left[-\frac{1}{T(r)}\left(\varphi(r,z) - \varphi(r,0)\right)\right] \quad , \tag{23}$$

where the normalization is determined by the measured quantity $Q(r) = A\int dz\ n(r,z)$. The constant A is determined by the collimator hole size and by absolute calibrations of the amplifier gains and capacitances. Using this expression for $n(r,z)$ in Poisson's equation and invoking the known boundary conditions on the cylindrical wall allows one to solve for the potential and density as a function of r and z. Fig. 6 shows an example of calculated level curves for the electron density.

Fig. 7 shows $n(r, z = 0)$ for three different times. One can see that the profile is evolving toward a shape that looks to be of the thermal equilibrium form. The same figure also shows the rotation frequency,

$$\omega(r,0) = \frac{v_\theta(r,0)}{r} = \frac{c}{B}\left[\frac{\partial\varphi}{\partial r} - \frac{1}{ne}\frac{\partial}{\partial r}(nT)\right] \quad , \tag{24}$$

calculated from data taken at $t = 0$, 0.5, and 2 sec. The initially injected plasma has substantial shear, but one can see that the plasma has evolved to a state which is near rigid rotation (thermal equilibrium) by $t = 2$ sec. After this time, the plasma profile evolves more slowly, presumably due to small external torques.

In this manner, we make a rough estimate of the time for transport to thermal equilibrium. Fig. 8 shows a log log plot of this time versus

magnetic field strength. The line which scales as B^2 is determined by estimating the transport time according to the new theory, and the line which scales like B^4 is determined in the same manner by the traditional theory. One can see that the evolution times are consistent with the new theory while being up to 10^3 times shorter than predicted by the traditional theory. The large error bars in Fig. 8 should be taken seriously. The data does not prove a scaling of the form $\tau \propto B^2$, but suggests a scaling somewhere between $\tau \propto B^{1.5}$ and $B^{2.5}$. Further, there are unwanted systematic variations in both plasma density and temperature as the magnetic field is changed, and the effects of these variations have not been removed from the scaling data. Of course, the results do not prove that the new theory is correct; they are too limited in scope for that; but they are thus far consistent with the new theory.

Future experimental data should provide incisive tests of the new theory. In principle, we obtain a complete description of the plasma, and we should be able to compare the measured flux $\Gamma_r(r)$ to the measured shears in the velocity $v_\theta(r)$. If the transport is the result of "local" viscosity, we will obtain the viscosity coefficient directly, for comparison to Eqs. (13) and (16).

V. Acknowledgment

This work is supported by NSF grant PHY83-06077 and ONR contract N00014-82K-0621.

VI. References

1. T.M. O'Neil and C.F. Driscoll, Phys. Fluids 22, 266 (1979); S.A. Prasad and T.M. O'Neil, Phys. Fluids 22, 278 (1983); J.H. Malmberg and T.M. O'Neil, Phys. Rev. Lett. 39, 1077 (1977).

2. C.F. Driscoll, K.S. Fine, and J.H. Malmberg, Bull. Am. Phys. Soc. 30, 1552 (1985).

3. A. Simon, Phys. Rev. 100, 1557 (1955).

4. C.L. Longmire and M.N. Rosenbluth, Phys. Rev. 103, 507 (1956).

5. T.M. O'Neil, Phys. Rev. Lett. 55, 943 (1985).

6. D.H.E. Dubin, T.M. O'Neil, and C.F. Driscoll, "Transport Toward Thermal Equilibrium of a Pure Electron Plasma," Proceedings of the US-Japan Workshop on Statistical Plasma Physics (Nagoya, Japan, 1986).

7. C.F. Driscoll, K.S. Fine, and J.H. Malmberg, Phys. Fluids 29, 2015 (1986).

8. J.H. Malmberg, T.M. O'Neil, A.W. Hyatt, and C.F. Driscoll, Proceedings of the 1984 Sendai Symposium on Plasma Nonlinear Phenomena (Tohoku U.P., Sendai, Japan, 1984), p. 31.

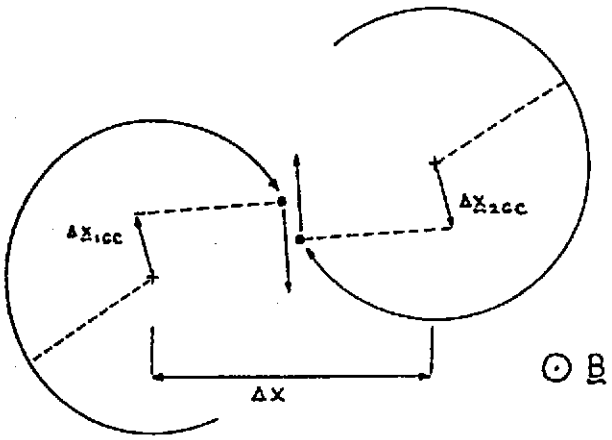

Fig. 1. A collision in the traditional theory. Electron and initial guiding center positions are given by dots and crosses, respectively.

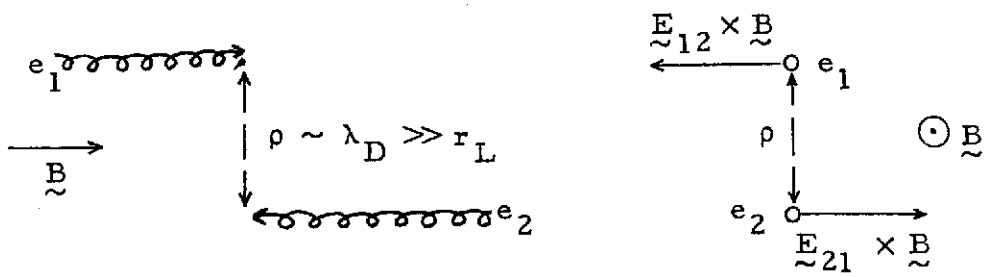

Fig. 2. Side view and end view of collision in the new theory. The electrons experience equal and opposite $\underset{\sim}{E} \times \underset{\sim}{B}$ drifts.

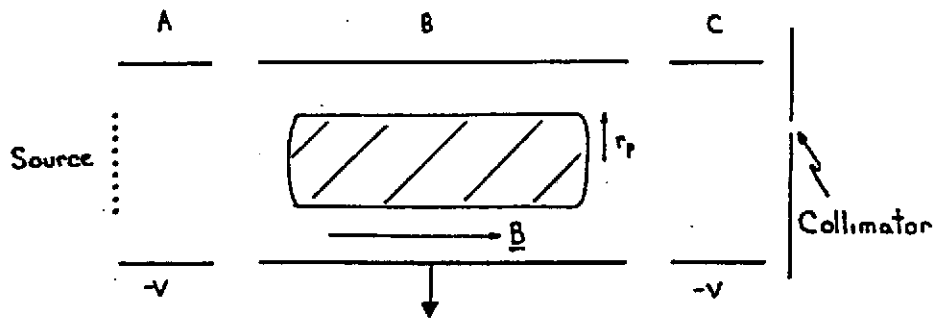

Fig. 3. Schematic diagram of plasma containment device.

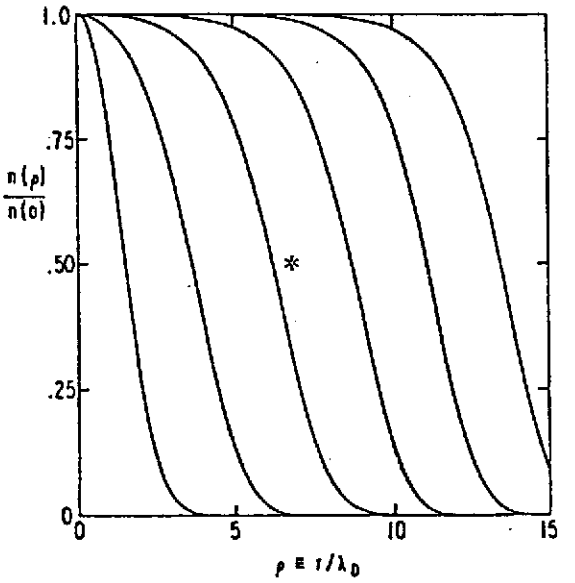

Fig. 4. Theoretical prediction of thermal equilibrium density profiles for given ω, T and varying N. The asterisk marks the profile which is closest to the experimental parameters.

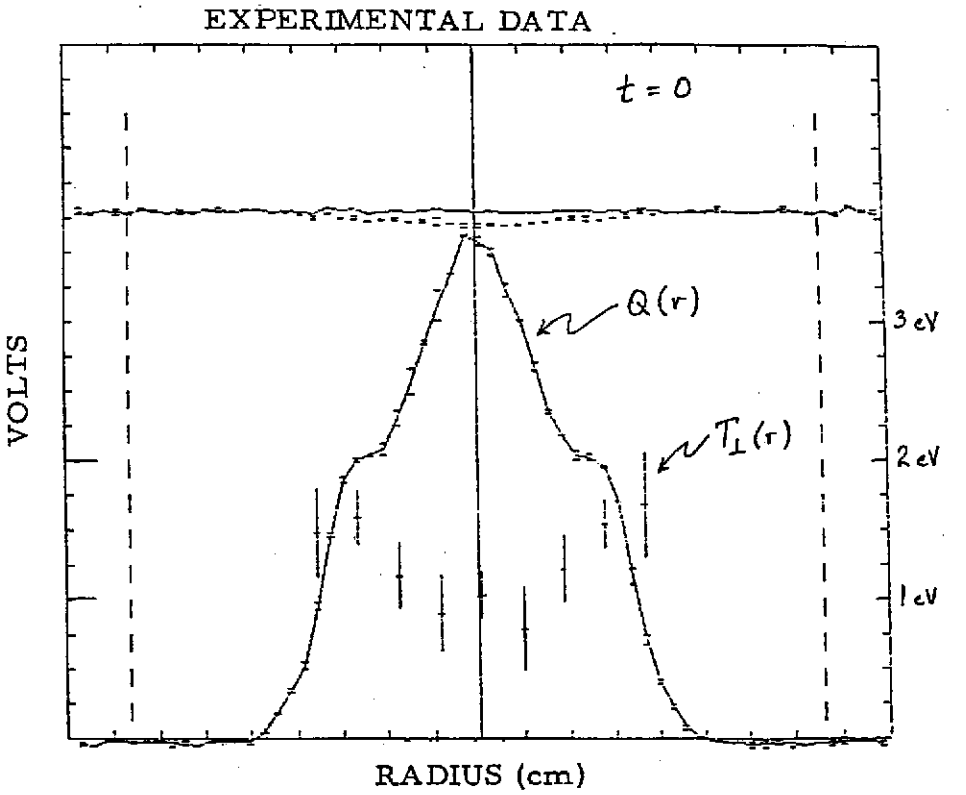

Fig. 5. Measured charge (number of electrons) on field lines passing through collimator and temperature of electrons on these lines as a function of the radial position of the collimator.

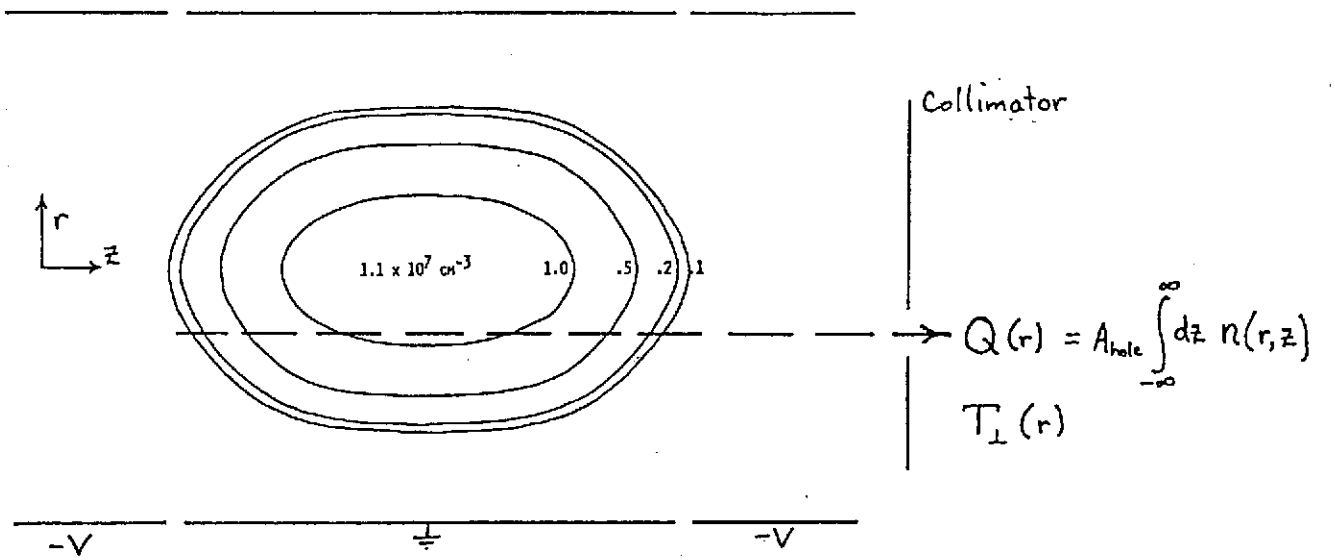

Fig. 6. Contour plots of n(r, z) at a particular time.

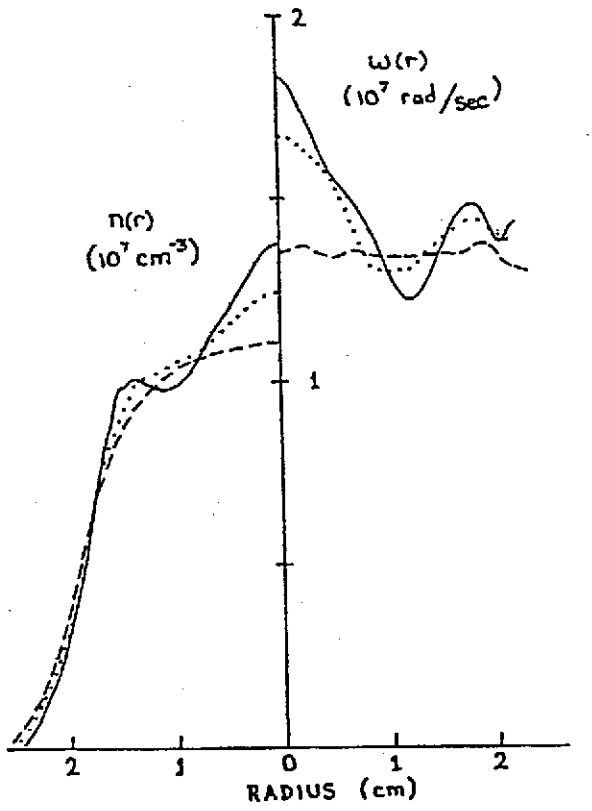

Fig. 7. Density and rotation frequency profiles at 3 different times. Solid curves: immediately after plasma formation (t = 0). Dotted curves: t = 0.5 sec. Dashed curves: t = 2 sec.

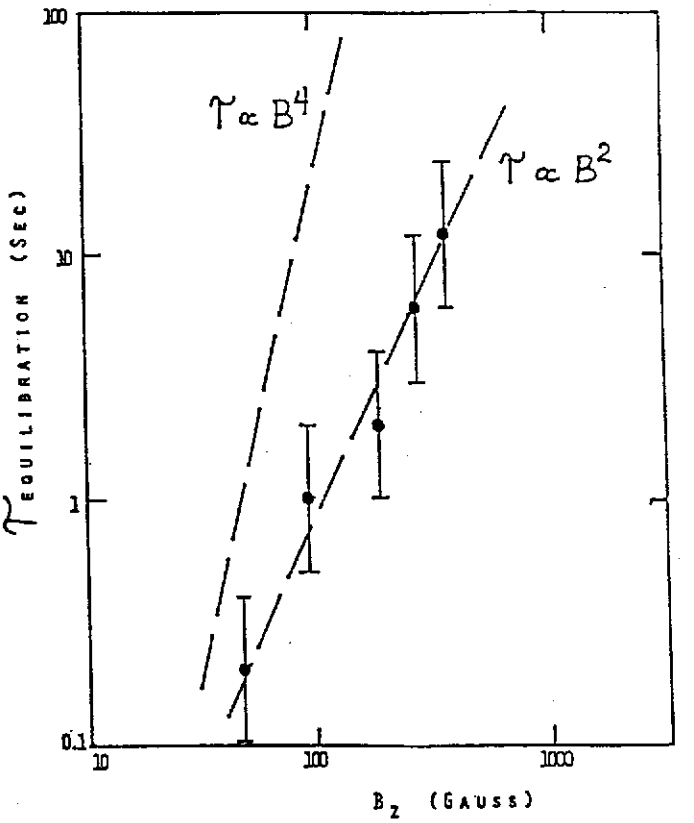

Fig. 8. Scaling of equilibration time τ with magnetic field. Dots are experimental points. Dashed lines show that τ scales like B^2 rather than B^4.